Extreme Glacier Melt on the Central Tibetan Plateau during the Summer of 2022: Detection and Mechanisms

Fei Zhu[1,2], Meilin Zhu[3]*, Lu An[1,2]

[1]College of Surveying and Geo-Informatics, Tongji University, Shanghai, 200092, China.

[2]Center for Spatial Information Science and Sustainable Development, Tongji University, Shanghai, 200092, China.

[3]Center for the Pan-Third Pole Environment, Lanzhou University, Lanzhou 730000, China.

Corresponding author: Meilin Zhu* (zhuml@lzu.edu.cn)

Table S1. List of the model parameters, range of parameters used to estimate the uncertainties in melt during extreme heat events and mass balance on Sangqu Glacier at glacier scale.

parameter	Value	+/-	Sensitivity in melt (mm w.e.)
a_{snow}	0.94	0.03	61.7
a_{firn}	0.75	0.03	20.9
a	-0.3	10%	0
b	0.48	10%	32.1
$T_{snow/rain}$(°C)	8.6	10%	0.6
P(%/100m)	18.8	10%	-1.9
C_b	0.01	10%	-6.1
K	0.0062	10%	-21.8
S_{in}_K	0.974	0.01	-5.1
T_lapse_rate (°C/100m)	0.6	0.1	-63.6
E_k	-	10%	-9.9
C_{eff}	-	10%	10.5

Table S2. List of the model parameters, range of parameters used to estimate the uncertainties in mass balance during 2019/20 on Sangqu Glacier at glacier scale.

parameter	Value	+/-	Sensitivity in mass balance (mm w.e.)
a_{snow}	0.94	0.03	124.1
a_{firn}	0.75	0.03	117.1
a	-0.3	10%	-1.4
b	0.48	10%	77.8
$T_{snow/rain}$(°C)	8.6	10%	-0.3
P(%/100m)	18.8	10%	-7.3
C_b	0.01	10%	6.4
K	0.0062	10%	-38.6
S_{in}_K	0.974	0.01	-15.4
T_lapse_rate (°C/100m)	0.6	0.1	-126.6
E_k	-	10%	-6.3
C_{eff}	-	10%	6.5

Table S3. List of the model parameters, range of parameters used to estimate the uncertainties in mass balance during 2020/21 on Sangqu Glacier at glacier scale.

parameter	Value	+/-	Sensitivity in mass balance (mm w.e.)
a_{snow}	0.94	0.03	113.5
a_{firn}	0.75	0.03	133.8
a	-0.3	10%	-0.4
b	0.48	10%	183.7
$T_{snow/rain}$(℃)	8.6	10%	1.8
P(%/100m)	18.8	10%	2.2
C_b	0.01	10%	22.7
K	0.0062	10%	-57.9
S_{in}_K	0.974	0.01	-28.5
T_lapse_rate (℃/100m)	0.6	0.1	-134.2
E_k	-	10%	-14.6
C_{eff}	-	10%	14.2

Table S4. List of the model parameters, range of parameters used to estimate the uncertainties in mass balance during 2021/22 on Sangqu Glacier at glacier scale.

parameter	Value	+/-	Sensitivity in mass balance (mm w.e.)
a_{snow}	0.94	0.03	132
a_{firn}	0.75	0.03	93.3
a	-0.3	10%	0.8
b	0.48	10%	117.4
$T_{snow/rain}$(℃)	8.6	10%	-0.2
P(%/100m)	18.8	10%	-1.4
C_b	0.01	10%	-4.2
K	0.0062	10%	-68.4
S_{in}_K	0.974	0.01	-16.9
T_lapse_rate (℃/100m)	0.6	0.1	-163.3
E_k	-	10%	-9.9
C_{eff}	-	10%	10.5

K is turbulent flux coefficient. C_b is background turbulent exchange coefficient. S_{in}_K is a constant, for which values are typically in the range 0.87–1.00, depending on the geographic position. E_k is effective thermal conductivity. C_{eff} is heat capacity.

Table S5. June–August SHI and circulation indices for 2020–2022

Year	SHI (ERA5)	SHI(tuotuohe)	GTI	NSI
2020	1.666	-	-1.254	-0.033
2021	1.863	1.288	0.361	0.244
2022	1.782	1.684	-0.117	2.123

Note: Negative GTI indicates weaker westerlies; positive NSI indicates northward displacement of the SAH.

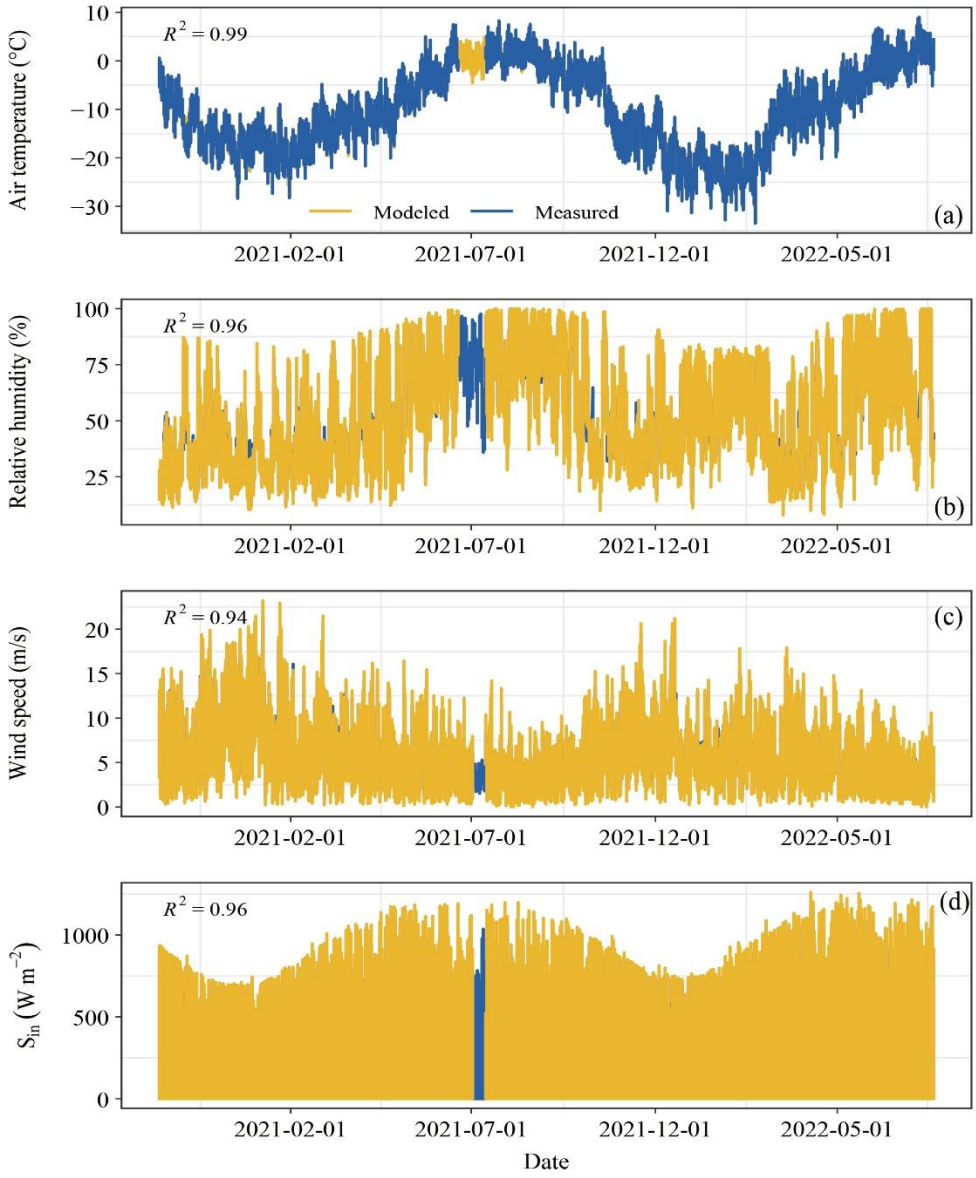


Figure S1. Comparison of observed and ERA5 downscaled (a) Air temperature, (b) Relative humidity, (c) Wind speed, and (d) Incoming shortwave radiation at the daily scale.

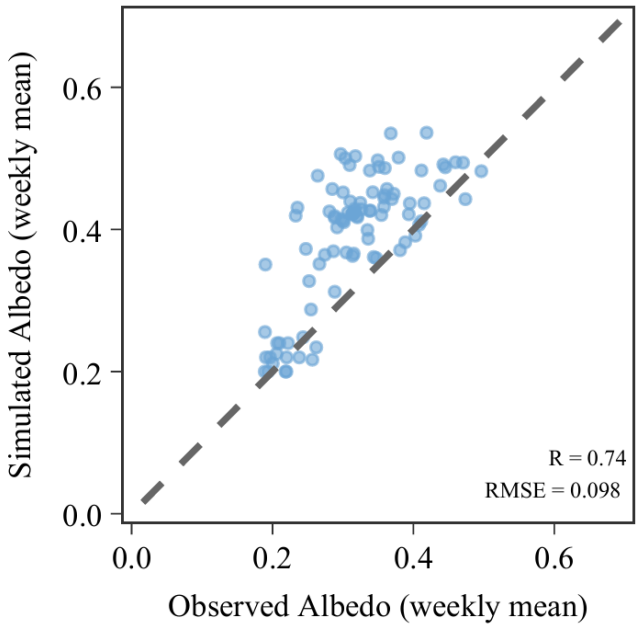


Figure S2. Comparison of albedo at weekly scale at the AWS site on Sangqu Glacier.

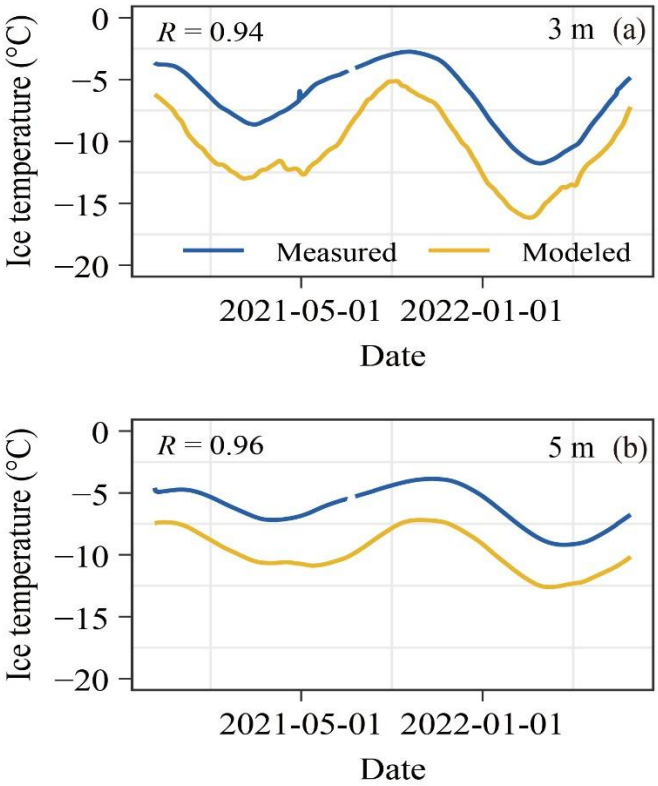


Figure S3. Comparison of observed and simulated ice temperatures at (a) 3 m and (b) 5 m.

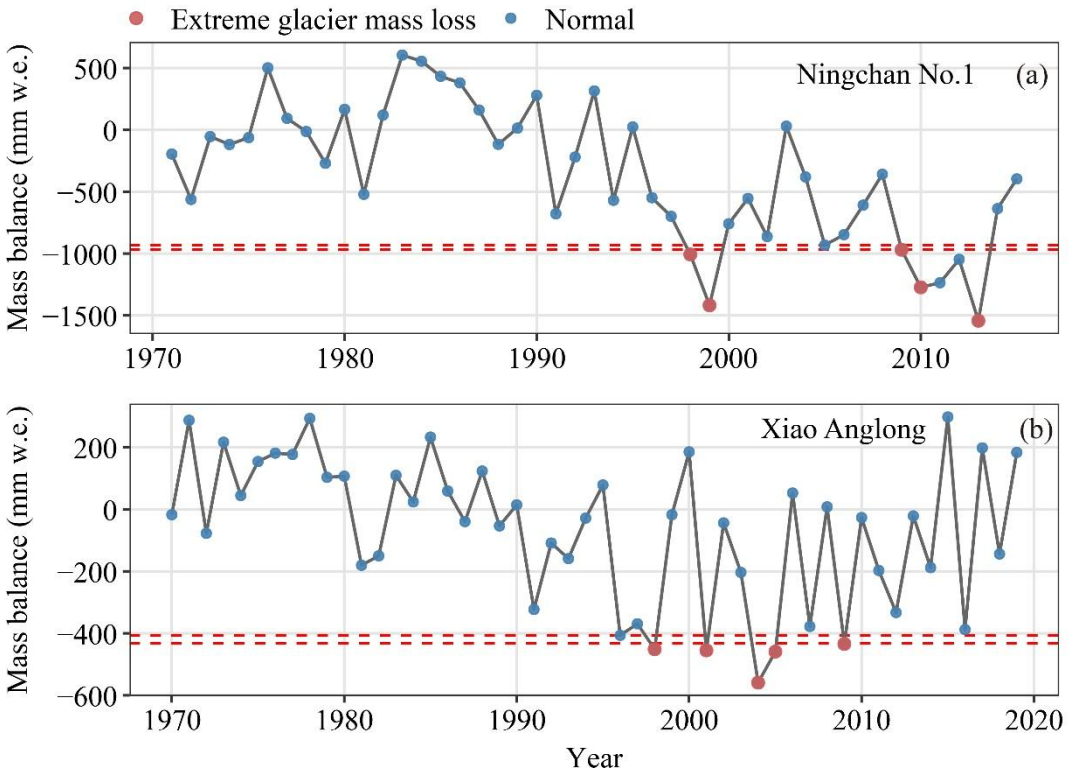


Figure S4. Annual mass balance time series and extreme mass loss events for (a) Ningchan No.1 Glacier and (b) Xiao Anglong Glacier. The data were sourced from Zhu et al. (2021, 2022). The red dashed line indicates the threshold for identifying extreme mass loss events.

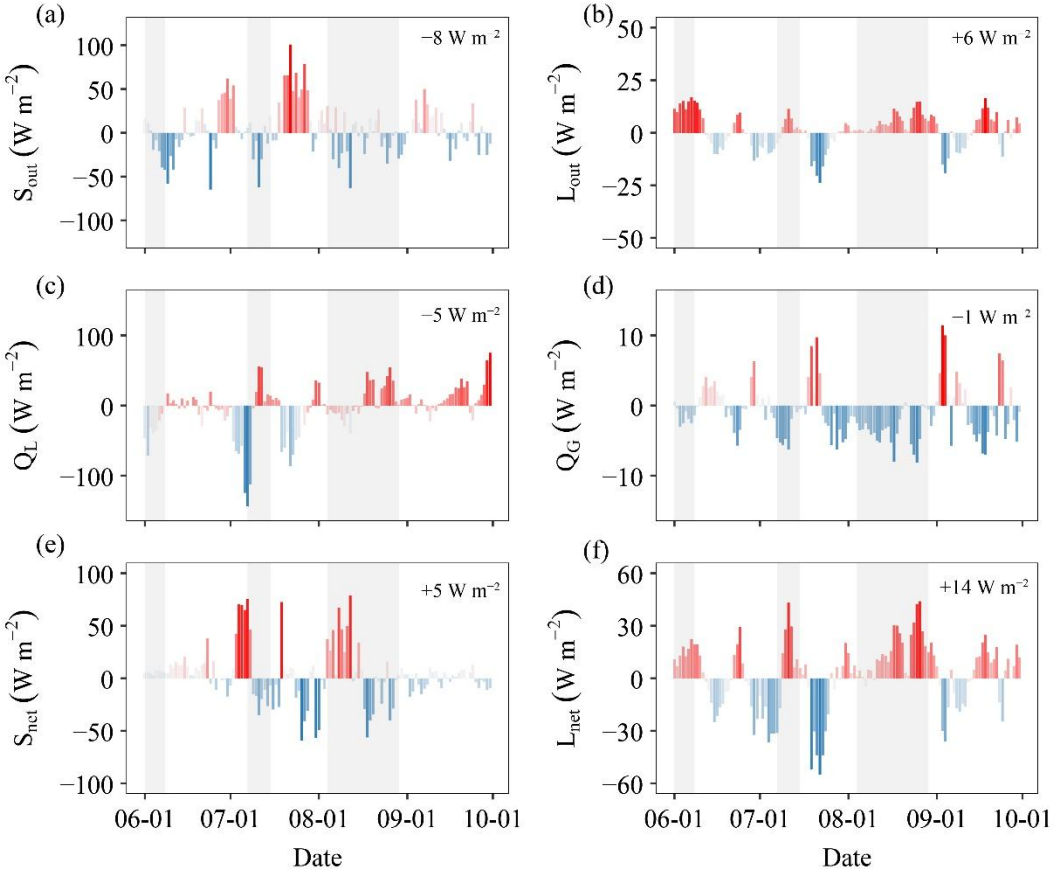


Figure S5. Glacier-wide energy balance anomalies associated with the extreme melt events. Anomalies in (a) outgoing shortwave radiation, (b) outgoing longwave radiation, (c) latent heat flux, (d) snow/ice heat flux, (e) net shortwave radiation, and (f) net longwave radiation are shown relative to the reference period October 2019–September 2021. Gray shading indicates the 2022 summer heatwave period (June–September).

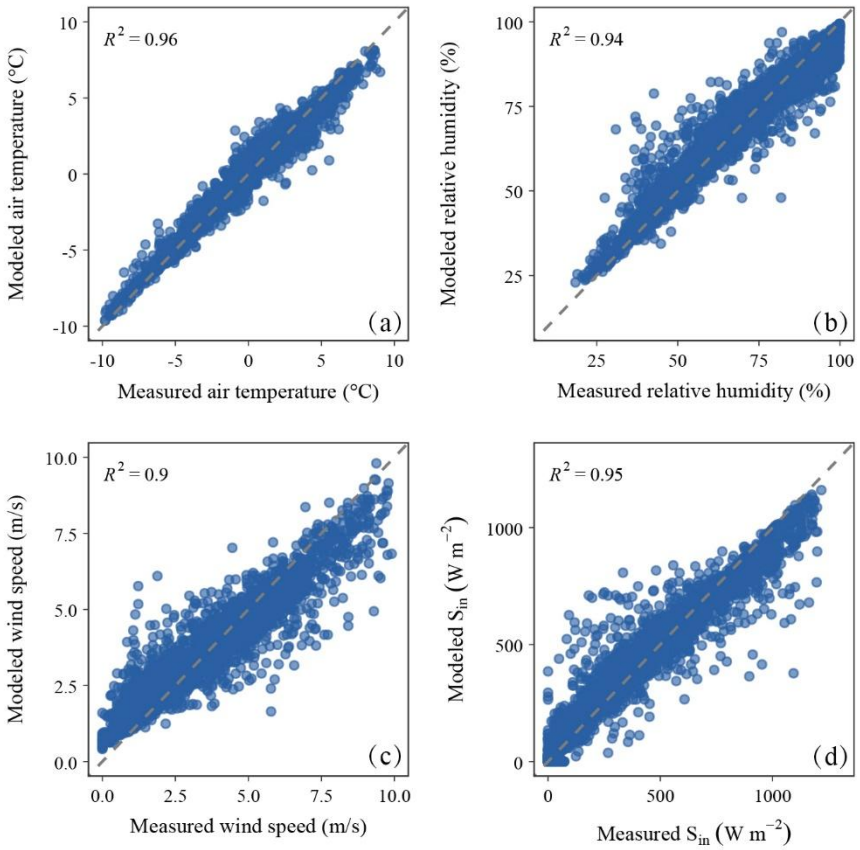


Figure S6. Comparison of observed and ERA5 downscaled (a) air temperature, (b) relative humidity, (c) wind speed, and (d) incoming shortwave radiation at the daily scale during the ablation season (June–September).

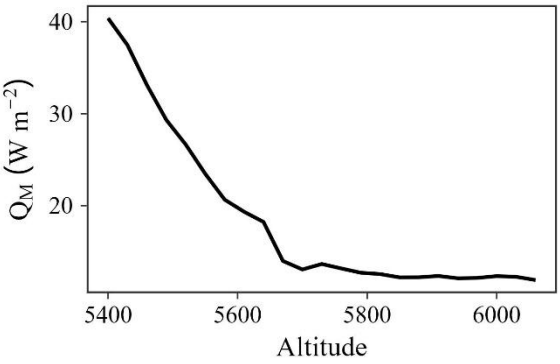


Figure S7. Melt energy versus elevation for the 2021–2022 mass balance year.

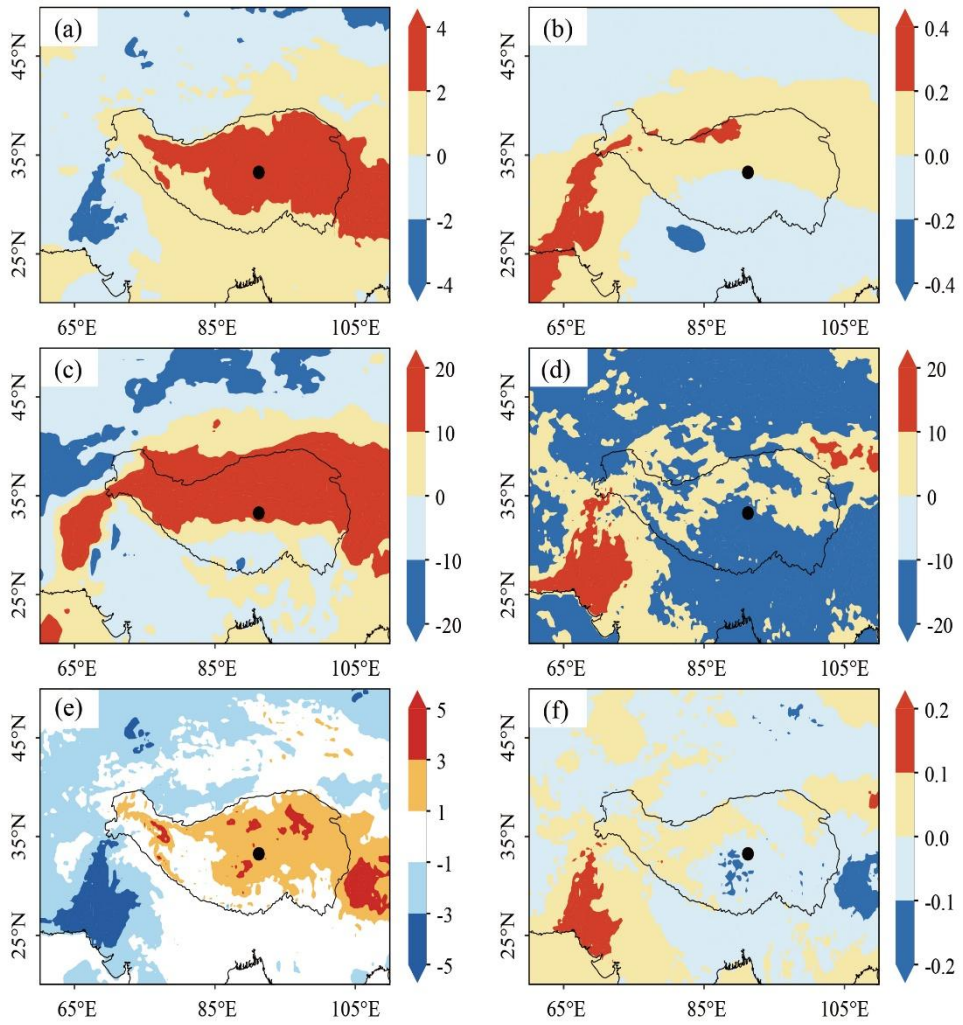


Figure S8. Anomalies in (a) air temperature, (b) cloud cover, (c) incoming longwave radiation, (d) sensible heat flux, (e) soil temperature, and (f) soil moisture during the summer 2022 heatwave (reference period: 1992–2021).

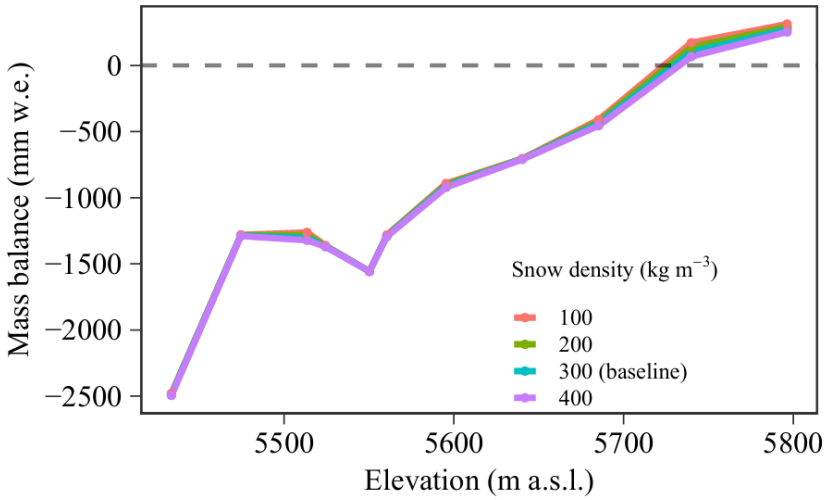


Figure S9. Sensitivity of point mass balance to snow density at different elevations for the 2019/20 mass balance year.

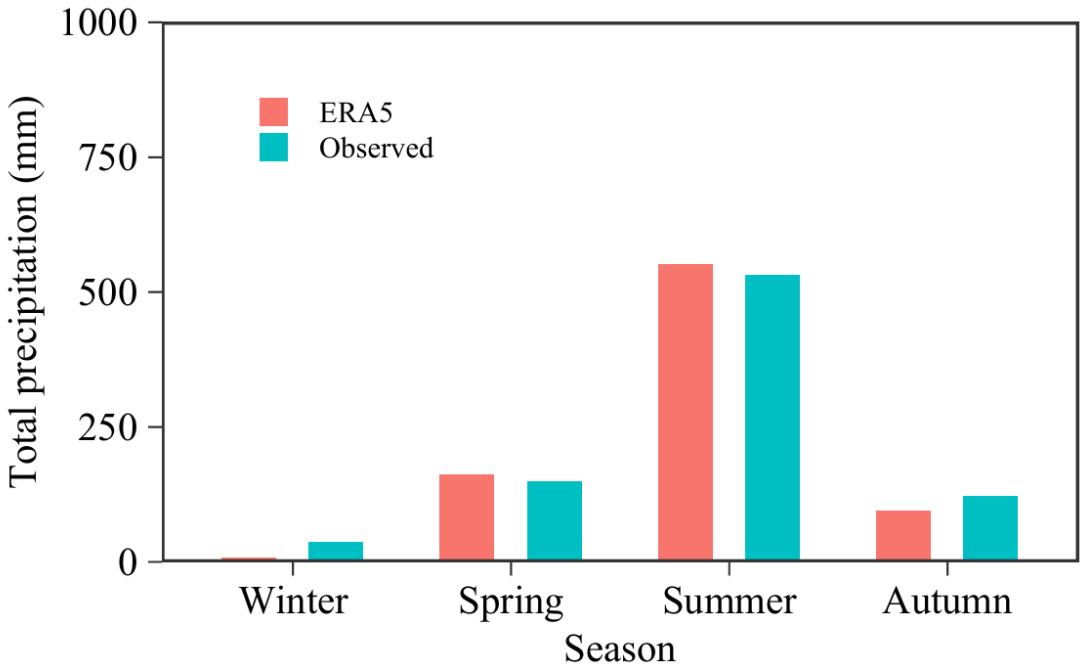


Figure S10. Seasonal comparison between ERA5 and in-situ precipitation measurements at Sangqu Glacier.

References

Dussaillant, I., Hugonnet, R., Huss, M., Berthier, E., Bannwart, J., Paul, F., and Zemp, M.: Annual mass change of the world's glaciers from 1976 to 2024 by temporal downscaling of satellite data with in situ observations, Earth Syst. Sci. Data, 17, 1977–2006, https://doi.org/10.5194/essd-17-1977-2025, 2025.

Zhu, M., Thompson, L. G., Zhao, H., Yao, T., Yang, W., and Jin, S.: Influence of atmospheric circulation on glacier mass balance in western Tibet: an analysis based on observations and modeling, J. Clim., 1–55, https://doi.org/10.1175/JCLI-D-20-0988.1, 2021.

Zhu, M., Yao, T., Thompson, L. G., Wang, S., Yang, W., and Zhao, H.: What induces the spatiotemporal variability of glacier mass balance across the Qilian Mountains, Clim Dyn, 59, 3555–3577, https://doi.org/10.1007/s00382-022-06283-4, 2022.